Classification: Biological Sciences, Neuroscience

Title: Motor pathway convergence predicts vocal learning capacities in oscine birds

Author affiliations:

Jordan M. Moore[a,1], Tamás Székely[b], József Büki[c], and Timothy J. DeVoogd[d]

[a]Department of Neurobiology and Behavior, Cornell University, Ithaca, NY 14853; [b]Department of Biology and Biochemistry, University of Bath, Bath, BA2 7AY UK; [c]Hungarian Ornithological Institute, Budapest, H-1121 Hungary; [d]Department of Psychology, Cornell University, Ithaca, NY 14853

[1]Corresponding author:

Jordan Moore

Dept. of Psychology, Columbia University

252 Schermerhorn Hall

1190 Amsterdam Ave.

New York, NY 10027

Phone: 212-854-5452

E-mail: jmm256@cornell.edu

Abstract

Behavioral specializations are frequently associated with expansions of brain regions controlling them. Examples of these relationships span sensory, motor, and cognitive abilities and are found across a wide variety of species, suggesting that they represent a general principle of vertebrate brain evolution. Yet, the precise mechanisms by which increases in neuron number underlie behavioral elaborations have seldom been identified and whether this concept can be extrapolated to entire neural pathways is unknown. Birdsong is a complex, learned motor behavior that varies immensely across species but is controlled by an evolutionarily conserved and discrete neural circuit. Using phylogenetic comparative methods, we show that the capacity to learn multiple song components is strongly related to the amount of descending control along the song motor pathway and that syllable repertoire size is more accurately predicted by pathway convergence than by its overall number of neurons. Furthermore, the degrees of convergence along serial premotor and primary motor projections are unrelated to each other and account for distinct portions of the behavioral variation. These findings suggest that selection on different aspects of song has driven changes in distinct components of this hierarchical motor pathway. They also elucidate a straightforward mechanism by which evolutionary increases in descending motor control could have underlied increases in birdsong repertoire size.

\body

Introduction

Many behavioral capacities are directly related to the size of the brain regions controlling them. Examples of these associations are found throughout the vertebrate lineage and include structures involved in sensory processing [e.g., visual (1-3), auditory (4, 5), olfactory (1, 4, 6), and somatosensory (7)]; sensorimotor integration and motor coordination (8-10); and complex

cognitive tasks such as spatial memory (11-13), procedural learning (14), and possibly human language (15). These relationships are generally thought to exist because larger brain regions possess greater computational power and/or exert greater influence over other areas (16), but the precise physiological mechanisms underlying them have rarely been identified (17). Most analyses have also been limited to one or a few brain areas, therefore it remains unknown how behavioral capacities relate to aspects of neural circuit structure beyond overall size.

Birdsong is a learned vocal communication signal characterized by tremendous interspecific diversity. Species vary especially in their capacity to learn multiple song components, ranging from those that learn only a single syllable (18) to others that can produce repertoires of thousands of distinct sounds (19). The neural basis of this variation likely lies within the song system, a discrete and conserved network dedicated to song learning and production (Fig. 1; 20, 21). Two parallel pathways that arise from premotor nucleus HVC constitute the majority of this circuit: a caudal motor pathway controls song production (22, 23) and a rostral, basal ganglia loop mediates song learning and plasticity but is not required for song production in adults (24-27).

Three lines of evidence suggest that the size of nucleus HVC is a principal determinant of the capacity to learn large repertoires. First, repertoire size and HVC volume are positively correlated within species (28, 29), between species (30, 31), and between sexes (32, 33). Second, they co-vary after experimental treatments that enhance (34) or constrain (35) song learning. HVC volume is unaffected by withholding song exposure during development, however, therefore its size more likely reflects the amount of learning possible than the amount of learning accomplished (36-38). Third, the potential physiological basis for this relationship was identified in the zebra finch (*Taeniopygia guttata*): HVC sparsely encodes temporal features

of song whereby individual premotor neurons fire a single, precisely-timed burst of action potentials during each song rendition (23). If this specificity between single neurons and brief song segments is general across species (39), then evolutionary increases in repertoire size would seem to require corresponding increases in HVC neuron number.

The significance of the HVC-repertoire association remains contentious, however, because HVC volume usually explains a small proportion of the behavioral variation and large outliers can dominate the correlations (40). Moreover, some species in which males and females sing equivalent repertoires have dimorphic HVC volumes (41, 42); age-related increases in repertoire size can occur without increases in HVC volume (43); and seasonal fluctuations in HVC volume are not always accompanied by changes in repertoire size (44-46). These observations seem to contradict notions of a strict correspondence between the two. Here, we investigate whether the consideration of multiple song nuclei improves this relationship and describe an aspect of song system architecture that accurately predicts syllable repertoire size across a wide phylogeny of species.

Results

Relationships between song nuclei

All anatomical and behavioral measurements are provided in Dataset S1 of the online supporting information. Phylogenetic comparative analyses were based on a composite phylogeny constructed from published molecular studies (Fig. 2). Each song nucleus volume scaled positively with the telencephalon but they differed in their variability (Table S1). HVC and MMAN, in particular, had very weak allometric relationships ($0.31 \leq r^2 \leq 0.34$). The volumes of RA, Area X, LMAN, and nXIIts scaled more directly with the telencephalon ($0.40 \leq$

$r^2 \leq 0.50$), and Uva and DM sizes tightly corresponded to it ($0.72 \leq r^2 \leq 0.76$). These differences were especially apparent in comparisons of absolute volumes between similarly-sized species. For example, the spotted flycatcher (*Muscicapa striata*) had HVC and MMAN volumes that were 15- and 9-fold larger, respectively, than those of the common yellowthroat (*Geothlypis trichas*), but it had RA, Area X, and LMAN volumes that were only 3-4 times as large (Fig. S1). Despite this heterogeneity, strong positive correlations still linked most song nucleus volumes after accounting for overall size (Table S2).

Neural correlates of syllable repertoire size

Results from multiple phylogenetic generalized least squares (PGLS) models that explained variation in syllable repertoire size as a function of various song nucleus volume combinations are provided in Table S3. A full model that included all song nuclei as predictor variables accounted for a large proportion of the behavioral variation (R^2 = 0.72; AIC = 57.4). Three reduced models containing nuclei along the caudal motor pathway were comparable: HVC, RA, nXIIts (R^2 = 0.71; AIC = 49.8; likelihood ratio test (LRT) P = 0.80); HVC and RA (R^2 = 0.67; AIC = 54.1; LRT P = 0.19), and HVC and nXIIts (R^2 = 0.67; AIC = 53.9; LRT P = 0.20). Inclusion of interaction terms did not improve the predictive value of any of these models. A surprising pattern emerged among the partial coefficients of these and many other reduced models: the slope associated with the most afferent nucleus (relative to the syrinx) was positive while those describing efferent area(s) were usually negative. For instance, the coefficients for MMAN and HVC were nearly always positive, that for nXIIts was generally negative, and those for intermediate nuclei such as RA and Area X were contingent upon the nucleus with which they were paired (i.e. positive when paired with an efferent nucleus but negative when with an afferent nucleus). The only exception was HVC, which always retained a positive coefficient.

These opposing relationships suggested that motor pathway convergence, defined as the size of HVC relative to RA [$HVC_{(RA)}$] and RA relative to nXIIts [$RA_{(nXIIts)}$], would be a superior predictor of song learning capacities than their volumes relative to the telencephalon. This was illustrated with residual analyses (Fig. 3, Table S4). Syllable repertoire size was more strongly related to $HVC_{(RA)}$ (r^2 = 0.61; AIC = 58.4) than to HVC relative to the telencephalon (r^2 = 0.44; AIC = 76.3), and it was significantly related to $RA_{(nXIIts)}$ (r^2 = 0.22; AIC = 92.3) but not to the volumes of either RA or nXIIts relative to the telencephalon (both $P > 0.08$). Interestingly, $HVC_{(RA)}$ and $RA_{(nXIIts)}$ were not correlated (r = 0.24, P = 0.10) and both retained significant, positive partial coefficients [2.6 ($P < 0.0001$) and 1.4 (P = 0.0009), respectively] in a two-factor model explaining the variation in repertoire size (R^2 = 0.69; AIC = 48.6). This model was significantly better than one based on the entire song motor pathway volume relative to the telencephalon (R^2 = 0.31; AIC = 85.9). The same patterns emerged from analyses of song motor pathway neuron numbers (#). $HVC\#_{(RA\#)}$ and $RA\#_{(nXIIts\#)}$ were strongly associated with repertoire size (R^2 = 0.63; AIC = 57.3; Table S5), were a significantly better predictor of it than overall pathway neuron number (R^2 = 0.40; AIC = 79.2), and were not related to each other (r = 0.07; P = 0.64). These measures seem likely to reflect genuine differences in the number of descending fibers along these pathways because HVC and RA neuron numbers were inversely related to RA and nXIIts neuronal densities, respectively, after accounting for overall telencephalon size (both $r < -0.42$; both $P < 0.001$).

Syllable repertoire size was only related to HVC and MMAN (both $P \leq 0.0002$) when song nuclei were considered individually (Table S6), and it was not related to any of the areas outside the song system: telencephalon (r = 0.18, P = 0.21), M (r = -0.08, P = 0.59), Hp (r = -0.11, P = 0.45), Sep (r = -0.06, P = 0.70), TnA (r = -0.12, P = 0.43), or MLd (r = 0.02, P = 0.88).

Discussion

As songbirds diversified, changes in syllable repertoire size closely paralleled those in the degree of song motor pathway convergence. Surprisingly, distinct portions of the observed behavioral variation are attributable to serial premotor and primary motor projections, $HVC_{(RA)}$ and $RA_{(nXIIts)}$, respectively. This suggests a modular organization whereby selection on particular song features has shaped the structure of distinct song motor pathway components. It also implies that increases in the amount of descending motor control, and not global circuit expansions, have led to greater song learning capacities because the volumes of RA and nXIIts are *inversely* related to the residuals from the HVC- and RA-repertoire regressions, respectively. In other words, species with fewer HVC and RA neurons than expected from their repertoire also have relatively few RA and nXIIts neurons, respectively, while those with more HVC and RA neurons than expected from their repertoire have correspondingly high RA and nXIIts neuron numbers. Thus, even though the song system has evolved as a cohesive network with strong positive correlations linking most relative nucleus volumes, the ability to learn many syllables is more accurately predicted by the relative size differences between nuclei than by their collective size relative to the rest of the brain.

New syllables could be created in at least two ways: by modifying the sequence and/or temporal properties of brief sounds already mastered or by producing novel, acoustically distinct sounds. Physiological studies in the zebra finch illuminate how increases in $HVC_{(RA)}$ and $RA_{(nXIIts)}$ could accomplish these feats. HVC-to-RA projection neurons sparsely encode song whereby each cell fires a short (~6 ms), temporally precise burst of action potentials that corresponds to one specific song segment (23). These cells are thought to be connected via axon

collaterals to form a feedforward synfire chain, whereby the sequential firing of neurons along a chain specifies an entire syllable or song (47-51). Pools of neurons that are simultaneously active would then excite unique ensembles of RA neurons, for which population-level activity patterns also correspond to short song segments (52, 53). Expansions of $HVC_{(RA)}$ could enable the production of larger repertoires in at least two ways. First, they would enhance syntactical capacities by increasing the number of possible synfire chains within HVC. Even if many of the neurons share the same projection patterns onto a given number of RA neurons, this would increase the number of ways to combine short sounds. Alternatively, more HVC-to-RA neurons with distinct projection patterns would excite novel RA ensembles and could lead to the generation of new sounds (see below). As an extension of this notion, smaller $HVC_{(RA)}$ sizes would limit both the number of possible synfire chains and the number of potential RA ensembles and thereby constrain a bird's syntactic and/or acoustic flexibility.

Individual RA neurons are less specific and burst multiple times throughout each song rendition, but population-level activity patterns are as temporally precise as those in HVC and also correspond to specific syllable segments (52, 53). RA represents the first myotopic map of syringeal and respiratory muscles along this pathway (54, 55), and its activity patterns affect song phonology because the adduction or abduction of syringeal labia and the airflow past them largely shape the spectral features of song (56). It has been suggested that the strength of each muscular contraction is determined by the linear sum of RA inputs onto nXIIts neurons rather than the specific composition of the RA ensembles (53, 57). If true and if RA axon arborization and synaptic strengths are relatively constant, increases in $RA_{(nXIIts)}$ would increase the total amount of excitatory input received by each nXIIts neuron, expand its range of attainable firing rates, and thus increase the potential contractile strength of that motor unit. On the other hand, if

increases in $RA_{(nXIIts)}$ are accompanied by decreases in RA axonal branching and/or synaptic strengths, increases in convergence could facilitate more precise and smaller changes in nXIIts firing rates. Either of these scenarios would enable greater control over syringeal shape and could thereby lead to the production of more spectrally varied sounds.

Of course, species likely vary in numerous other ways that impact these relationships. Approximately half of all HVC neurons project to RA in the zebra finch (58, 59), but this may not be representative of other species. Other potential variables include axonal arborization patterns, synaptic strengths and densities, motor unit size, syringeal muscle number, and physiological activity patterns. Differences in song can further complicate comparisons between species, such as when syllables differ in their degree of difficulty. Nevertheless, the relationship between repertoire size and motor pathway convergence is robust and current models of song encoding provide a potential explanation as to why it exists (53, 57).

Many species organize syllables into distinct song types or vary their sequence in predictable ways. The brain area(s) underlying this higher order song patterning have not been identified, but they seem likely to be afferent to HVC given the hierarchical organization of the song system. MMAN appears particularly well situated to serve such a role insofar as the extensive behavioral variability can be expected to accompany large anatomical differences. Its axons ramify throughout HVC (60) and its relative volume is both highly variable across species and strongly correlated with that of HVC. Moreover, MMAN lesions made in juvenile zebra finches severely disrupt song learning and prevent song stabilization. Those made in adults have more modest effects but do increase syntactical variability, especially the identity of a song's first syllable (61). Future experiments in species capable of learning multiple song types will help to clarify MMAN's role in song production.

It has long been thought that heightened behavioral capacities emerge due to broad expansions of the neural circuits controlling them. Our results support this view on the whole but also reveal informative aspects of circuit architecture overlooked by this explanation. In particular, we demonstrate that relative size differences between circuit components can be a superior indicator of behavioral abilities than the overall number of neurons in the pathway. Other motor systems may be structured in a similar way. The connectivity of the song system closely resembles that of a movement-associated motor network in birds (62), and it seems plausible that similar physiological mechanisms encode both types of behaviors. Differences in manual dexterity across mammals are also ostensibly related to the degree of convergence along the corticospinal tract (63-66). Such wide-ranging comparisons are limited in many ways, but the available evidence suggests that motor pathway convergence may relate to several capacities in addition to birdsong. These findings refine the common belief that behavioral specializations are related to gross expansions of their underlying neural substrate and highlight the importance of descending neural control in the evolution of a learned motor behavior.

Materials and Method

Specimen collection and preparation

One to four adult male songbirds of 58 temperate zone species spanning 18 families were wild-caught with mist nets. Collections were restricted to spring months (April – June) when birds were reproductively active to minimize seasonal variation in song system anatomy. Most were collected throughout Hungary from 1993-1995 or in Tompkins County, New York in 2004. Exceptions were the white-throated sparrows (*Zonotrichia albicollis*) from Ontario, Canada in 1991; European pied flycatchers (*Ficedula hypoleuca*) from central Norway in 1995; yellow-

throated buntings (*Emberiza elegans*) from China in 1991; and northern mockingbirds (*Mimus polyglottos*) from North Carolina in 2003. At the time of capture, birds were deeply anesthetized with a barbiturate anesthetic and transcardially perfused with 0.8% saline followed by 10% formalin in saline. Brains were extracted, post-fixed for at least 24 hours, cryoprotected with 30% sucrose/10% formalin, embedded in gelatin, and sectioned at 40 μm in the coronal plane with a sliding microtome. Sections were then mounted onto gel-coated slides and Nissl-stained with cresyl violet. All appropriate local, provincial, and/or national permits were held at the time of bird collection, and all procedures were approved by the Cornell University Institutional Animal Care and Use Committee.

Brain measurements

Nucleus and brain region boundaries were traced with aid of a camera lucida from every other section viewed with 40× or from every fourth section viewed with 20× magnification [mesopallium and hippocampus only]. The telencephalon was measured in every fourth section from unmagnified digital images. All reported values are from one side of the brain, typically the left except in cases where torn tissue or poor staining prevented measurements of that side. Cross-sectional areas of scanned boundary traces and telencephalon images were measured with NIH ImageJ software (67) and final volumes were computed by summing the areas and multiplying by the sampling interval (0.08 or 0.16 mm).

Exemplar images of each nucleus and additional delineation criteria are provided in the online supporting information (Fig. S2). The song nuclei measured include HVC, the robust nucleus of the arcopallium (RA), Area X of the striatum, the lateral and medial magnocellular nuclei of the anterior nidopallium (LMAN and MMAN, respectively), uvaeformis (Uva), the dorsomedial nucleus of the intercollicular complex (DM), and the tracheosyringeal portion of the

hypoglossal nucleus (nXIIts). The boundaries of most were unambiguous. HVC traces included the two subdivisions visible in coronal sections: a central region that contains large, darkly-stained cells and a caudomedial region (i.e. paraHVC) comprised of small, densely-packed neurons (68). In most cases, MMAN and LMAN were easily distinguished; when they were contiguous, their shared boundary was delineated on the basis of MMAN's slightly smaller somata. Song nuclei that could not be reliably identified in all specimens were not measured included the nucleus interface of the nidopallium (NIf), the medial portion of the dorsolateral nucleus of the anterior thalamus (DLM), and the dorsomedial nucleus of the posterior thalamus (DMP). Other brain regions analyzed included the mesopallial subdivision of the telencephalon (M), which has been related to feeding innovation rate (69); limbic structures involved in spatial memory (hippocampus (Hp), 70), territoriality and sociality (septum (Sep), 71, 72), or sexual behavior and pair bonding (nucleus taeniae of the amygdala (TnA), 73, 74); and an auditory nucleus (dorsal part of the lateral mesencephalic nucleus (MLd), 75). Specimens representing 13 of the 58 species were used in previous studies (30, 31, 76); all areas were re-measured and exclusion of these data did not alter the principal findings reported here.

Neuronal densities in HVC, RA, and nXIIts were estimated from one brain of each species. Presumptive neurons were discriminated from glia on the basis of their larger somata, uniformly stained cytoplasm, and single nucleolus. Nucleolus counts were made using sampling windows evenly distributed throughout each structure and, on average, 13 tallies (range: 7-26) were made in each. Grid dimensions were 80 × 80 μm (600×, HVC and nXIIts) or 120 × 120 μm (400×, RA).

Syllable repertoires

The behavioral unit of interest was a song syllable, defined as a continuous trace on a spectrogram or a stereotyped sequence of notes separated by less than 25 msec. A syllable repertoire is the number of unique syllables produced by an individual bird. Species-typical syllable repertoires were obtained for 49 of the 58 species, mostly from published sources (provided in the online supporting information). When multiple sources were found for a species, one was chosen on the basis of sample size, conformity of the syllable definition with that above, proximity of the recording site to the site of specimen collection, and the season during which recordings were made.

Repertoires for seven species were estimated from recordings held by the Macaulay Library at Cornell University using the Syrinx sound analysis program (77). All syllables known to originate from one individual were used to construct plots of new syllables encountered versus the total number of syllables sampled. The function $y = a(1 - e^{-bx})$ was fit to the data and the asymptote (a) was used as the estimated repertoire and averaged across individuals for each species.

Phylogeny

A fully resolved, composite phylogeny was constructed from published molecular phylogenies (Fig. 2; sources provided in the online supporting information). All inter-family relationships were inferred from the analysis of two nuclear genes (RAG-1 and RAG-2). Most intra-family relationships were based on the mitochondrial gene(s) cytochrome *b* and/or ND2, occasionally in addition to a nuclear gene. Given this diversity of methods, arbitrary branch lengths were used for statistical analyses.

Comparative analysis

We used Mesquite v2.5 (78) to manage data and trees and the PDAP:PDTree v1.14 module to analyze independent contrasts (79, 80). We constructed phylogenetic generalized least squares (PGLS) models with the Matlab program REGRESSIONv2.m (81) after converting the phylogenetic tree to a variance-covariance matrix with the PDDIST module of the Phenotypic Diversity Analysis Programs (80).

Analyses were based on $\log_{10}$-transformed data. In all cases, we used the arbitrary branch lengths of Grafen (82) scaled with the rho transform (ρ = 0.3) because this tree passed the diagnostic tests for all traits (83, 84). Results from conventional statistics that disregard phylogenetic relatedness (i.e. assume a star phylogeny) were qualitatively consistent but are not reported here. We constructed numerous PGLS models to (1) explore the relationships between relative song nucleus volumes and (2) explain the variation in syllable repertoire size as a function of various brain measurements. Because behavioral data were only available from 49 species, the latter analyses were run after the phylogenetic tree was pruned, branch lengths re-scaled and diagnostic tests re-run. Nested and non-nested models were compared using ln maximum likelihood ratio tests (LRTs) and the Akaike Information Criterion (AIC; smaller is better), respectively. Partial *F*-tests were used to determine the significance of independent variable parameters in multivariate models. Note that R^2 values from PGLS models are not comparable to those from traditional ordinary least squares models.

A 'size' covariate was included in every model, but the actual measurement used depended on the particular analysis. When the variable of interest was a telencephalic nucleus or subdivision, we used the difference between the telencephalon and the respective system/subdivision volume (i.e. T – sum of song nuclei (T-SS), T – sum of limbic structures (T-LS), or T–M) in order to control for part-whole artifacts. Otherwise, telencephalon volume was

used as the 'size' covariate for analyses of MLd, and species-typical body mass (85) was used for analyses of the telencephalon.

We conducted residual analyses to illustrate the concept of 'pathway convergence,' but we call attention to the tendency for this procedure to yield biased parameter estimates (86, 87). Here, regression slopes were estimated for a $\log_{10}$-transformed nucleus volume as a function of the same 'size' reference above [e.g., log(HVC) versus log(T–SS)] or of another nucleus [e.g., log(HVC) versus log(RA)]. These slopes were then used to compute relative trait volumes with the formula $\log_{10}[\text{trait}/(\text{size}^{b})]$, where *b* was the regression exponent, and 'trait' and 'size' were original data values.

Acknowledgements

We thank the national and provincial authorities in Hungary and state and local authorities in New York for collection permits. We are grateful for specimens provided by Helene Lampe, Li Dongfeng, and Carlos Botero; assistance in the field by Hedwig Mezo; help with histology by Zachary Buchan and Joyce Reed; and statistical software by Theodore Garland. We thank D.H. Bhatt for providing helpful comments on an earlier version of this manuscript. Funding was provided by NSF Grant 0090963 (TJD), the US-Hungarian Joint Scientific Fund (JFNo. 117 to TJD and TS), and an NSFGRF (JMM).

References

1. Barton RA, Purvis A, Harvey PH (1995) Evolutionary radiation of visual and olfactory brain systems in primates, bats and insectivores. *Phil Trans R Soc Lond B* 348:381-392.

2. Barton RA (2004) Binocularity and brain evolution in primates. *Proc Natl Acad Sci USA* 101:10113-10115.

3. Iwaniuk AN, Heesy CP, Hall MI, Wylie DRW (2008) Relative Wulst volume is correlated with orbit orientation and binocular visual field in birds. *J Comp Physiol A* 194:267-282.

4. Hutcheon JM, Kirsch JAW, Garland JT (2002) A comparative analysis of brain size in relation to foraging ecology and phylogeny in the Chiroptera. *Brain Behav Evol* 60:165-180.

5. Kubke MF, Massoglia DP, Carr CE (2004) Bigger brains or bigger nuclei? Regulating the size of auditory structures in birds. *Brain Behav Evol* 63:169-180.

6. Barton RA (2006) Olfactory evolution and behavioral ecology in primates. *Am J Primatol* 68:545-558.

7. Catania KC, Henry EC (2006) Touching on somatosensory specializations in mammals. *Curr Op Neurobiol* 16:467-473.

8. Barton RA, Dean P (1993) Comparative evidence indicating neural specialization for predatory behaviour in mammals. *Proc R Soc Lond B* 254:63-68.

9. Clark DA, Mitra PP, Wang SSH (2001) Scalable architecture in mammalian brains. *Nature* 411:189-193.

10. Iwaniuk AN, Wylie DRW (2007) Neural specialization for hovering in hummingbirds: hypertrophy of the pretectal nucleus lentiformis mesencephali. *J Comp Neurol* 500:211-221.

11. Krebs JR, Sherry DF, Healy SD, Perry VH, Vaccarino AL (1989) Hippocampal specialization of food-storing birds. *Proc Natl Acad Sci USA* 86:1388-1392.

12. Safi K, Dechmann DKN (2005) Adaptation of brain regions to habitat complexity: a comparative analysis in bats (Chiroptera). *Proc R Soc B* 272:179-186.

13. Shumway CA (2008) Habitat complexity, brain, and behavior. *Brain Behav Evol* 72:123-134.

14. Day LB, Westcott DA, Olster DH (2005) Evolution of bower complexity and cerebellum size in bowerbirds. *Brain Behav Evol* 66:62-72.

15. Rilling JK, et al. (2008) The evolution of the arcuate fasciculus revealed with comparative DTI. *Nat Neurosci* 11:426-428.

16. Striedter GF (2005) *Principles of Brain Evolution* (Sinauer Associates, Inc., Sunderland, MA).

17. Carr CE, Friedman MA (1999) Evolution of time coding systems. *Neural Comput* 11:1-20.

18. Liu WC, Kroodsma DE (1999) Song development by chipping sparrows and field sparrows. *Anim Behav* 57:1275-1286.

19. Kroodsma DE, Parker LD (1977) Vocal virtuosity in the brown thrasher. *Auk* 94:783-785.

20. Nottebohm F, Stokes TM, Leonard CM (1976) Central control of song in the canary, *Serinus canarius*. *J Comp Neurol* 165:457-486.

21. Nottebohm F, Kelley DB, Paton JA (1982) Connections of vocal control nuclei in the canary telencephalon. *J Comp Neurol* 207:344-357.

22. Vu ET, Mazurek ME, Kuo YC (1994) Identification of a forebrain motor programming network for the learned song of zebra finches. *J Neurosci* 14:6924-6934.

23. Hahnloser RHR, Kozhevnikov AA, Fee MS (2002) An ultra-sparse code underlies the generation of neural sequences in a songbird. *Nature* 419:65-70.

24. Bottjer SW, Miesner EA, Arnold AP (1984) Forebrain lesions disrupt development but not maintenance of song in passerine birds. *Science* 224:901-903.

25. Scharff C, Nottebohm F (1991) A comparative study of the behavioral deficits following lesions of various parts of the zebra finch song system: implications for vocal learning. *J Neurosci* 11:2896-2913.

26. Ölveczky BP, Andalman AS, Fee MS (2005) Vocal experimentation in the juvenile songbird requires a basal ganglia circuit. *PLoS Biol* 3:e153.

27. Kao MH, Doupe AJ, Brainard MS (2005) Contributions of an avian basal ganglia-forebrain circuit to real-time modulation of song. *Nature* 433:638-643.

28. Nottebohm F, Kasparian S, Pandazis C (1981) Brain space for a learned task. *Brain Res* 213:99-109.

29. Canady RA, Kroodsma DE, Nottebohm F (1984) Population differences in complexity of a learned skill are correlated with the brain space involved. *Proc Natl Acad Sci USA* 81:6232-6234.

30. DeVoogd TJ, Krebs JR, Healy SD, Purvis A (1993) Relations between song repertoire size and the volume of brain nuclei related to song: comparative evolutionary analyses amongst oscine birds. *Proc R Soc Lond B* 254:75-82.

31. Székely T, Catchpole CK, DeVoogd A, Marchl Z, DeVoogd TJ (1996) Evolutionary changes in a song control area of the brain (HVC) are associated with evolutionary changes in song repertoire among European warblers (Sylviidae). *Proc R Soc Lond B* 263:607-610.

32. Brenowitz EA, Arnold AP, Levin RN (1985) Neural correlates of female song in tropical duetting birds. *Brain Res* 343:104-112.

33. MacDougall-Shackleton SA, Ball GF (1999) Comparative studies of sex differences in the song-control system of songbirds. *Trends Neurosci* 22:432-436.

34. Markman S, et al. (2008) Pollutants increase song complexity and the volume of the brain area HVC in a songbird. *PLoS One* 3:e1674.

35. Spencer KA, Buchanan KL, Leitner S, Goldsmith AR, Catchpole CK (2005) Parasites affect song complexity and neural development in a songbird. *Proc R Soc B* 272:2037-2043.

36. Burek MJ, Nordeen KW, Nordeen EJ (1991) Neuron loss and addition in developing zebra finch song nuclei are independent of auditory experience during song learning. *J Neurobiol* 22:215-223.

37. Brenowitz EA, Lent K, Kroodsma DE (1995) Brain space for learned song in birds develops independently of song learning. *J Neurosci* 15:6281-6286.

38. Leitner S, Nicholson J, Leisler B, DeVoogd TJ, Catchpole CK (2002) Song and the song control pathway in the brain can develop independently of exposure to song in the sedge warbler. *Proc R Soc Lond B* 269:2519-2524.

39. Prather JF, Peters S, Nowicki S, Mooney R (2008) Precise auditory-vocal mirroring in neurons for learned vocal communication. *Nature* 451:305-310.

40. Bolhuis JJ, Macphail EM (2001) A critique of the neuroecology of learning and memory. *Trends Cogn Sci* 5:426-433.

41. Gahr M, Sonnenschein E, Wickler W (1998) Sex difference in the size of the neural song control regions in a dueting songbird with similar song repertoire size of males and females. *J Neurosci* 18:1124-1131.

42. Gahr M, Metzdorf R, Schmidl D, Wickler W (2008) Bi-directional sexual dimorphisms of the song control nucleus HVC in a songbird with unison song. *PLoS One* 3:e3073.

43. Nottebohm F, Nottebohm ME, Crane L (1986) Developmental and seasonal changes in canary song and their relation to changes in the anatomy of song-control nuclei. *Behav Neural Biol* 46:445-471.

44. Kirn JR, Clower RP, Kroodsma DE, DeVoogd TJ (1989) Song-related brain regions in the red-winged blackbird are affected by sex and season but not repertoire size. *J Neurobiol* 20:139-163.

45. Brenowitz EA, Nalls B, Wingfield JC, Kroodsma DE (1991) Seasonal changes in avian song nuclei without seasonal changes in song repertoire. *J Neurosci* 11:1367-1374.

46. Smith GT, Brenowitz EA, Wingfield JC, Baptista LF (1995) Seasonal changes in song nuclei and song behavior in Gambel's white-crowned sparrows. *J Neurobiol* 28:114-125.

47. Mooney R (2000) Different subthreshold mechanisms underlie song selectivity in identified HVc neurons of the zebra finch. *J Neurosci* 20:5420-5436.

48. Mooney R, Prather JF (2005) The HVC microcircuit: the synaptic basis for interactions between song motor and vocal plasticity pathways. *J Neurosci* 25:1952-1964.

49. Li MR, Greenside H (2006) Stable propagation of a burst through a one-dimensional homogeneous excitatory chain model of songbird nucleus HVC. *Phys Rev E* 74:011918.

50. Jin DZ, Ramazanoğlu FM, Seung HS (2007) Intrinsic bursting enhances the robustness of a neural network model of sequence generation by avian brain area HVC. *J Comput Neurosci* 23:283-299.

51. Long MA, Fee MS (2008) Using temperature to analyse temporal dynamics in the songbird motor pathway. *Nature* 456:189-194.

52. Yu AC, Margoliash D (1996) Temporal hierarchical control of singing in birds. *Science* 273:1871-1875.

53. Leonardo A, Fee MS (2005) Ensemble coding of vocal control in birdsong. *J Neurosci* 25:652-661.

54. Vicario DS (1991) Organization of the zebra finch song control system: II. Functional organization of outputs from nucleus *robustus archistriatalis*. *J Comp Neurol* 309:486-494.

55. Wild JM (1993) Descending projections of the songbird nucleus robustus archistriatalis. *J Comp Neurol* 338:225-241.

56. Goller F, Suthers RA (1996) Role of syringeal muscles in controlling the phonology of bird song. *J Neurophysiol* 76:287-300.

57. Fee MS, Kozhevnikov AA, Hahnloser RHR (2004) Neural mechanisms of vocal sequence generation in the songbird. *Ann NY Acad Sci* 1016:153-170.

58. Wang N, Aviram R, Kirn JR (1999) Deafening alters neuron turnover within the telencephalic motor pathway for song control in adult zebra finches. *J Neurosci* 19:10554-10561.

59. Ward BC, Nordeen EJ, Nordeen KW (2001) Anatomical and ontogenetic factors producing variation in HVc neuron number in zebra finches. *Brain Res* 904:318-326.

60. Foster EF, Mehta RP, Bottjer SW (1997) Axonal connections of the medial magnocellular nucleus of the anterior neostriatum in zebra finches. *J Comp Neurol* 382:364-381.

61. Foster EF, Bottjer SW (2001) Lesions of a telencephalic nucleus in male zebra finches: influences on vocal behavior in juveniles and adults. *J Neurobiol* 46:142-165.

62. Feenders G, et al. (2008) Molecular mapping of movement-associated areas in the avian brain: a motor theory for vocal learning origin. *PLoS One* 3:e1768.

63. Heffner R, Masterton B (1975) Variation in form of pyramidal tract and its relationship to digital dexterity. *Brain Behav Evol* 12:161-200.

64. Heffner RS, Masterton RB (1983) The role of the corticospinal tract in the evolution of human digital dexterity. *Brain Behav Evol* 23:165-183.

65. Nudo RJ, Masterton RB (1990) Descending pathways to the spinal cord, IV: Some factors related to the amount of cortex devoted to the corticospinal tract. *J Comp Neurol* 296:584-597.

66. Bortoff GA, Strick PL (1993) Corticospinal terminations in two new-world primates: further evidence that corticomotoneuronal connections provide part of the neural substrate for manual dexterity. *J Neurosci* 13:5105-5118.

67. Rasband WS (2007) *ImageJ, v1.38x*. US National Institutes of Health.

68. Fortune ES, Margoliash D (1995) Parallel pathways and convergence onto HVc and adjacent neostriatum of adult zebra finches (*Taeniopygia guttata*). *J Comp Neurol* 360:413-441.

69. Timmermans S, Lefebvre L, Boire D, Basu P (2000) Relative size of the hyperstriatum ventrale is the best predictor of feeding innovation rate in birds. *Brain Behav Evol* 56:196-203.

70. Healy SD, de Kort SR, Clayton NS (2005) The hippocampus, spatial memory and food hoarding: a puzzle revisited. *Trends Ecol Evol* 20:17-22.

71. Goodson JL, Eibach R, Sakata J, Adkins-Regan E (1999) Effect of septal lesions on male song and aggression in the colonial zebra finch (*Taeniopygia guttata*) and the territorial field sparrow (*Spizella pusilla*). *Behav Brain Res* 98:167-180.

72. Goodson JL, Evans AK, Wang Y (2006) Neuropeptide binding reflects convergent and divergent evolution in species-typical group sizes. *Horm Behav* 50:223-236.

73. Thompson RR, Goodson JL, Ruscio MG, Adkins-Regan E (1998) Role of the archistriatal nucleus taeniae in the sexual behavior of male Japanese quail (*Coturnix japonica*): A comparison of function with the medial nucleus of the amygdala in mammals. *Brain Behav Evol* 51:215-229.

74. Svec LA, Licht KM, Wade J (2009) Pair bonding in the female zebra finch: a potential role for the nucleus taeniae. *Neuroscience* 160:275-283.

75. Woolley SMN, Casseday JH (2005) Processing of modulated sounds in the zebra finch auditory midbrain: responses to noise, frequency sweeps, and sinusoidal amplitude modulations. *J Neurophysiol* 94:1143-1157.

76. DeVoogd TJ, Houtman AM, Falls JB (1995) White-throated sparrow morphs that differ in song production rate also differ in the anatomy of some song-related brain areas. *J Neurobiol* 28:202-213.

77. Burt JM (2006) *Syrinx, v2.6h*. http://www.syrinxpc.com/.

78. Maddison WP, Maddison DR (2008) *Mesquite: a modular system for evolutionary analysis, v2.5*. http://mesquiteproject.org/.

79. Garland T, Jr, Midford PE, Ives AR (1999) An introduction to phylogenetically based statistical methods, with a new method for confidence intervals on ancestral values. *Am Zool* 39:374-388.

80. Garland T, Jr, Ives AR (2000) Using the past to predict the present: confidence intervals for regression equations in phylogenetic comparative methods. *Am Nat* 155:346-364.

81. Lavin SR, Karasov WH, Ives AR, Middleton KM, Garland T, Jr. (2008) Morphometrics of the avian small intestine compared with that of nonflying mammals: a phylogenetic approach. *Physiol Biochem Zool* 81:526-550.

82. Grafen A (1989) The phylogenetic regression. *Phil Trans R Soc Lond B* 326:119-157.

83. Garland T, Jr, Harvey PH, Ives AR (1992) Procedures for the analysis of comparative data using phylogenetically independent contrasts. *Syst Biol* 41:18-32.

84. Blomberg SP, Garland T, Jr, Ives AR (2003) Testing for phylogenetic signal in comparative data: behavioral traits are more labile. *Evolution* 57:717-745.

85. Dunning JB (2008) *Handbook of avian body masses, 2nd ed.* (CRC Press, Boca Raton, FL).

86. Darlington RB, Smulders TV (2001) Problems with residual analysis. *Anim Behav* 62:599-602.

87. Freckleton RP (2002) On the misuse of residuals in ecology: regression of residuals vs. multiple regression. *J Anim Ecol* 71:542-545.

Figure Legends

Fig. 1. Major projections of the song system. The caudal motor pathway (black) underlies song production, the anterior forebrain pathway (gray) is required for song learning and plasticity, and feedback projections (dashed lines) coordinate activity between hemispheres. VRG: ventral respiratory group.

Fig. 2. Composite phylogeny of 58 species spanning 18 families used in this study. Arbitrary branch lengths were scaled with the method of Grafen (82) and the rho transform (ρ = 0.3). Sources are provided in the online supporting information.

Fig. 3. Correlations between standardized independent contrasts of $\log_{10}$(syllable repertoire) and (*a*) HVC volume relative to the telencephalon – song system [$HVC_{(T\text{-}SS)}$], (*b*) HVC volume relative to RA [$HVC_{(RA)}$], and (*c*) RA volume relative to nXIIts [$RA_{(nXIIts)}$]. Black and open symbols highlight the largest positive and negative deviations, respectively, in (*a*) and their reduction in (*b*). $N = 48$.

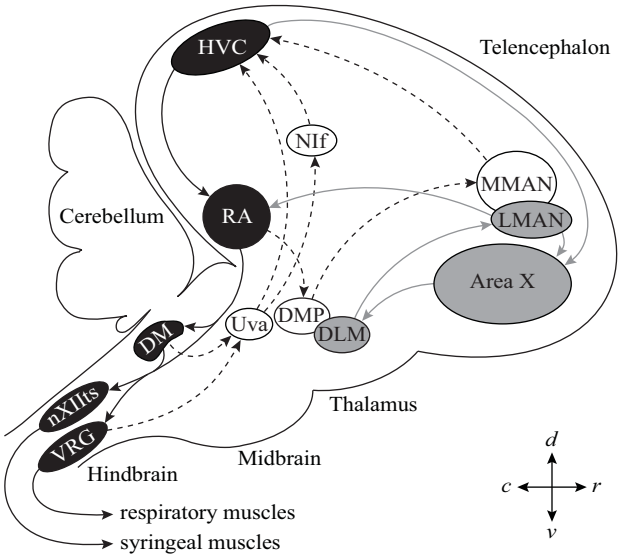
HVC
Telencephalon
NIf
MMAN
Cerebellum
RA
LMAN
Area X
Uva
DMP
DLM
DM
nXIIts
VRG
Thalamus
Midbrain
Hindbrain
respiratory muscles
syringeal muscles
d
c
r
v

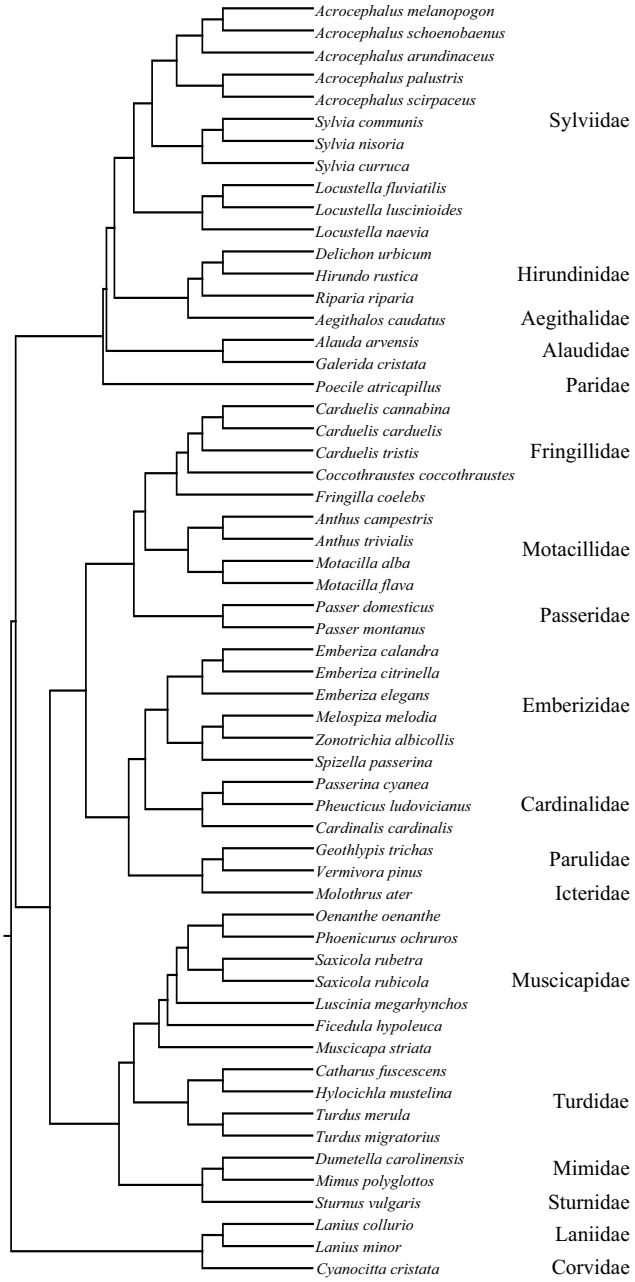
Acrocephalus melanopogon
Acrocephalus schoenobaenus
Acrocephalus arundinaceus
Acrocephalus palustris
Acrocephalus scirpaceus
Sylvia communis
Sylvia nisoria
Sylvia curruca
Locustella fluviatilis
Locustella luscinioides
Locustella naevia
Delichon urbicum
Hirundo rustica
Riparia riparia
Aegithalos caudatus
Alauda arvensis
Galerida cristata
Poecile atricapillus
Carduelis cannabina
Carduelis carduelis
Carduelis tristis
Coccothraustes coccothraustes
Fringilla coelebs
Anthus campestris
Anthus trivialis
Motacilla alba
Motacilla flava
Passer domesticus
Passer montanus
Emberiza calandra
Emberiza citrinella
Emberiza elegans
Melospiza melodia
Zonotrichia albicollis
Spizella passerina
Passerina cyanea
Pheucticus ludovicianus
Cardinalis cardinalis
Geothlypis trichas
Vermivora pinus
Molothrus ater
Oenanthe oenanthe
Phoenicurus ochruros
Saxicola rubetra
Saxicola rubicola
Luscinia megarhynchos
Ficedula hypoleuca
Muscicapa striata
Catharus fuscescens
Hylocichla mustelina
Turdus merula
Turdus migratorius
Dumetella carolinensis
Mimus polyglottos
Sturnus vulgaris
Lanius collurio
Lanius minor
Cyanocitta cristata
Sylviidae
Hirundinidae
Aegithalidae
Alaudidae
Paridae
Fringillidae
Motacillidae
Passeridae
Emberizidae
Cardinalidae
Parulidae
Icteridae
Muscicapidae
Turdidae
Mimidae
Sturnidae
Laniidae
Corvidae

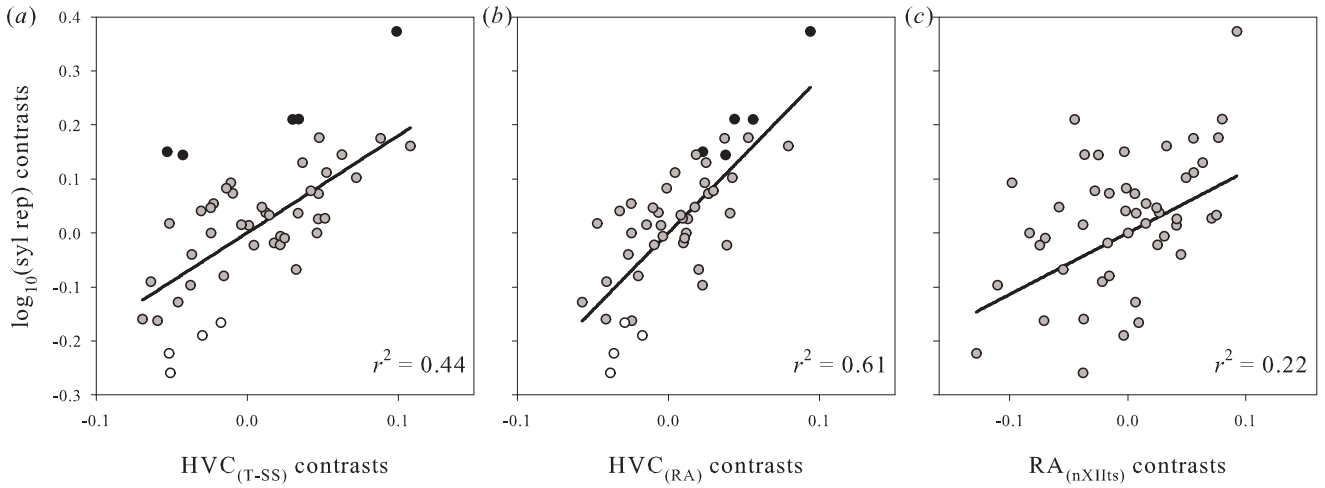
(a)
(b)
(c)
log10(syl rep) contrasts
0.4
0.3
0.2
0.1
0.0
-0.1
-0.2
-0.3
-0.1
0.0
0.1
r2 = 0.44
r2 = 0.61
r2 = 0.22
HVC(T-SS) contrasts
HVC(RA) contrasts
RA(nXIIts) contrasts

Moore et al.

Supporting Information

Fig. S1. Alternate coronal sections containing the left HVC and RA of a spotted flycatcher (*Muscicapa striata*) and common yellowthroat (*Geothlypis trichas*). The spotted flycatcher has approximately 15× more HVC neurons but only 3× more RA neurons than the common yellowthroat.

Fig. S2. Examples of the delineation criteria used for each nucleus in this study. Scale bar = 1 mm in each panel. (*a*) HVC, including both the central and caudomedial (paraHVC) subdivisions, of a marsh warbler (*Acrocephalus palustris*); (*b*) RA of a sand martin (*Riparia riparia*); (*c*) MMAN (red), LMAN (yellow), and Area X (green) of a northern wheatear (*Oenanthe oenanthe*); (*d*) Uva of a grey catbird (*Dumetella carolinensis*); (*e*) DM (red) and MLd (yellow) of a Eurasian skylark (*Alauda arvensis*); (*f*) nXIIts of a brown-headed cowbird (*Molothrus ater*); (*g*) Hp and Sep of a black-capped chickadee (*Poecile atricapillus*); (*h*) TnA of a common blackbird (*Turdus merula*).

SI Methods

Region delineation criteria

Rostral M was identified by differences in staining intensity compared to adjacent regions; in more central and caudal sections, it was clearly distinguished by the superior frontal and mesopallial laminae. The lateral extent of Hp was identified by its lower cell density compared to adjacent areas (1). Caudal Hp does not have a clear boundary with the surrounding parahippocampal area, therefore measurements were arbitrarily stopped at the section in which the cerebellum reached the dorsal-most extent of the telencephalon. Sep boundaries were identified by differences in staining intensity and appeared to coincide with those described by chemoarchitecture (2); the estimates reported here include most of the four major subdivisions but exclude portions of the nucleus of the diagonal band ventral to the

septopallio-mesencephalic tract. Both TnA and MLd were delineated on the basis of their staining intensity and/or cell density.

Syllable repertoire sources

Syllable repertoire sources listed in Dataset S1 are provided below (3-35). Sources used to construct the phylogeny were: inter-family (36); Sylviidae (37-40); Hirundinidae (41); Fringillidae (42-44); Motacillidae (45); Emberizidae (46, 47); Cardinalidae (48); Muscicapidae (49, 50); Turdidae (51); Mimidae (52).

References

1. Székely AD, Krebs JR (1996) Efferent connectivity of the hippocampal formation of the zebra finch (*Taenopygia guttata*): an anterograde pathway tracing study using *Phaseolus vulgaris leucoagglutinin*. *J Comp Neurol* 368:198-214.
2. Goodson JL, Evans AK, Lindberg L (2004) Chemoarchitectonic subdivisions of the songbird septum and a comparative overview of septum chemical anatomy in jawed vertebrates. *J Comp Neurol* 473:293-314.
3. Gill F, Wright M (2006) *Birds of the World: Recommended English Names* (Princeton University Press, Princeton, NJ).
4. Albrecht DJ, Oring LW (1995) Song in chipping sparrows, *Spizella passerina*: structure and function. *Anim Behav* 50:1233-1241.
5. Allan SE, Suthers RA (1994) Lateralization and motor stereotypy of song production in the brown-headed cowbird. *J Neurobiol* 25:1154-1166.
6. Anderson ME, Conner RN (1985) Northern cardinal song in three forest habitats in eastern Texas. *Wilson Bull* 97:436-449.

7. Bell BD, Borowiec M, Lontkowski J, Pledger S (2004) Short records of marsh warbler (*Acrocephalus palustris*) song provide indices that correlate with nesting success. *J Ornithol* 145:8-15.

8. Borror DJ (1965) Song variation in Maine song sparrows. *Wilson Bull* 77:5-37.

9. Briefer E, Aubin T, Lehongre K, Rybak F (2008) How to identify dear enemies: the group signature in the complex song of the skylark *Alauda arvensis*. *J Exp Biol* 211:317-326.

10. Buchanan KL, Catchpole CK (2000) Song as an indicator of male parental effort in the sedge warbler. *Proc R Soc Lond B* 267:321-326.

11. Catchpole CK (1980) Sexual selection and the evolution of complex songs among European warblers of the genus *Acrocephalus*. *Behaviour* 74:149-165.

12. Dobson CW, Lemon RE (1979) Markov sequences in songs of American thrushes. *Behaviour* 68:86-105.

13. Espmark YO, Lampe HM (1993) Variations in the song of the pied flycatcher within and between breeding seasons. *Bioacoustics* 5:33-65.

14. Falls JB, Kopachena JG (1994) in *Birds of North America Online,* ed. Poole, A. (Cornell Lab of Ornithology, Ithaca).

15. Feßl B, Hoi H (2000) Song complexity and song structure in the moustached warbler *Acrocephalus melanopogon*. *J Avian Biol* 31:144-150.

16. Forstmeier W, Hasselquist D, Bensch S, Leisler B (2006) Does song reflect age and viability? A comparison between two populations of the great reed warbler *Acrocephalus arundinaceus*. *Behav Ecol Sociobiol* 59:634-643.

17. Garamszegi LZ, et al. (2005) Estimating the complexity of bird song by using capture-recapture approaches from community ecology. *Behav Ecol Sociobiol* 57:305-317.

18. Gill FB, Murray BG (1972) Song variation in sympatric blue-winged and golden-winged warblers. *Auk* 89:625-643.

19. Güttinger HR, Clauss G (1982) Der gesangsaufbau von stieglitz-kanarienbastarden (*Carduelis carduelis* × *Serinus canaria*) im vergleich zu den elternarten. *J Ornithol* 123:269-286.

20. Hultsch H (1980) (Free University of Berlin), pp. 1-180.

21. Klit I (1999) The function of song forms in the lesser whitethroat *Sylvia curruca*. *Bioacoustics* 10:31-45.

22. Kroodsma DE, et al. (1999) Geographic variation in black-capped chickadee songs and singing behavior. *Auk* 116:387-402.

23. Kroodsma DE, Houlihan PW, Fallon PA, Wells JA (1997) Song development by grey catbirds. *Anim Behav* 54:457-464.

24. Lang AL, Barlow JC (1997) Cultural evolution in the Eurasian tree sparrow: divergence between introduced and ancestral populations. *Condor* 99:413-423.

25. Lemon RE, Chatfield C (1973) Organization of song of rose-breasted grosbeaks. *Anim Behav* 21:28-44.

26. Lemon RE, Struger J, Lechowicz MJ (1983) Song features as species discriminants in American warblers (Parulidae). *Condor* 85:308-322.

27. Nivison JJ (1978) (Wayne State University).

28. Ödeen A, Björklund M (2003) Dynamics in the evolution of sexual traits: losses and gains, radiation and convergence in yellow wagtails (*Motacilla flava*). *Mol Ecol* 12:2113-2130.

29. Payne RB (1981) Song learning and social interaction in indigo buntings. *Anim Behav* 29:688-697.

30. Schwager G, Güttinger HR (1984) Der gesangsaufbau von braunkehlchen (*Saxicola rubetra*) und schwarzkehlchen (*S. torquata*) im vergleich. *J Ornithol* 125:261-278.

31. Székely T, Catchpole CK, DeVoogd A, Marchl Z, DeVoogd TJ (1996) Evolutionary changes in a song control area of the brain (HVC) are associated with evolutionary changes in song repertoire among European warblers (Sylviidae). *Proc R Soc Lond B* 263:607-610.

32. Wahlström S (1966) En akustisk jämförelse mellan sången hos tre olika *Locustella*-arter. *Vår Fågelvärld* 25:161-166.

33. Wallschläger D (1964) A bioacoustical contribution to the systematics of th palearctic Motacillidae. I. Songs and call-notes of the genus *Anthus*. *Mitt Zool Mus Berl (Suppl)* 60:37-56.

34. Wildenthal JL (1965) Structure in primary song of the mockingbird (*Mimus polyglottos*). *Auk* 82:161-189.

35. Zeng SJ, et al. (2005) Song complexity is associated with the volume of brain song-control nuclei in ten oscine species. *Acta Zool Sinica* 51:68-75.

36. Barker FK, Cibois A, Schikler P, Feinstein J, Cracraft J (2004) Phylogeny and diversification of the largest avian radiation. *Proc Natl Acad Sci USA* 101:11040-11045.

37. Blondel J, Catzeflis F, Perret P (1996) Molecular phylogeny and the historical biogeography of the warblers of the genus *Sylvia* (Aves). *J Evol Biol* 9:871-891.

38. Leisler B, Heidrich P, Schulze-Hagen K, Wink M (1997) Taxonomy and phylogeny of reed warblers (genus *Acrocephalus*) based on mtDNA sequences and morphology. *J Ornithol* 138:469-496.

39. Helbig AJ, Seibold I (1999) Molecular phylogeny of palearctic-African *Acrocephalus* and *Hippolais* warblers (Aves: Sylviidae). *Mol Phylogenet Evol* 11:246-260.

40. Drovetski SV, et al. (2004) Mitochondrial phylogeny of *Locustella* and related genera. *J Avian Biol* 35:105-110.

41. Sheldon FH, Whittingham LA, Moyle RG, Slikas B, Winkler DW (2005) Phylogeny of swallows (Aves: Hirundinidae) estimated from nuclear and mitochondrial DNA sequences. *Mol Phylogenet Evol* 35:254-270.

42. Arnaiz-Villena A, et al. (2001) Phylogeography of crossbills, bullfinches, grosbeaks, and rosefinches. *Cell Mol Life Sci* 58:1159-1166.

43. Klicka J, Zink RM, Winker K (2003) Longspurs and snow buntings: phylogeny and biogeography of a high-latitude clade (*Calcarius*). *Mol Phylogenet Evol* 26:165-175.

44. Zamora J, et al. (2006) *Rhodopechys obsoleta* (desert finch): a pale ancestor of greenfinches (*Carduelis* spp.) according to molecular phylogeny. *J Ornithol* 147:448-456.

45. Arctander P, Folmer O, Fjeldså J (1996) The phylogenetic relationships of Berthelot's pipit *Anthus berthelotii* illustrated by DNA sequence data, with remarks on the genetic distance between rock and water pipits *Anthus spinoletta*. *Ibis* 138:263-272.

46. Klicka J, Burns K, Spellman GM (2007) Defining a monophyletic Cardinalini: a molecular perspective. *Mol Phylogenet Evol* 45:1014-1032.

47. Alström P, et al. (2008) Phylogeny and classification of the old world Emberizini (Aves, Passeriformes). *Mol Phylogenet Evol* 47:960-973.

48. Yuri T, Mindell DP (2002) Molecular phylogenetic analysis of Fringillidae, "new world nine-primaried oscines" (Aves: Passeriformes). *Mol Phylogenet Evol* 23:229-243.

49. Wink M, Sauer-Gürth H, Gwinner E (2002) Evolutionary relationships of stonechats and related species inferred from mitochondrial-DNA sequences and genomic fingerprinting. *Brit Birds* 95:349-355.

50. Voelker G, Spellman GM (2004) Nuclear and mitochondrial DNA evidence of polyphyly in the avian superfamily Muscicapoidea. *Mol Phylogenet Evol* 30:386-394.

51. Klicka J, Voelker G, Spellman GM (2005) A molecular phylogenetic analysis of the "true thrushes" (Aves: Turdinae). *Mol Phylogenet Evol* 34:486-500.

52. Cibois A, Cracraft J (2004) Assessing the passerine "tapestry": phylogenetic relationships of the Muscicapoidea inferred from nuclear DNA sequences. *Mol Phylogenet Evol* 32:264-273.

Table S1. Allometric relationships of song nuclei as a function of log(T-SS). In all cases, df = 56.

Nucleus	*r*	coef.	*t*	*P*
log(MMAN)	0.586	0.768	5.4157	<0.0001
log(Uva)	0.850	0.642	12.0677	<0.0001
log(HVC)	0.560	0.810	5.0538	<0.0001
log(Area X)	0.685	0.851	7.0302	<0.0001
log(LMAN)	0.631	0.793	6.0825	<0.0001
log(RA)	0.705	0.852	7.4322	<0.0001
log(DM)	0.869	0.634	13.1404	<0.0001
log(nXIIts)	0.647	0.669	6.3426	<0.0001

Table S2. Correlations between song nucleus volumes after accounting for the size covariate log(T-SS). Shaded cells indicate directly connected nuclei. In all cases, df = 55.

		log(MMAN)	log(Uva)	log(HVC)	log(Area X)	log(LMAN)	log(RA)	log(DM)
log(Uva)	*r*	0.047						
	F	0.120						
	P	0.730						
log(HVC)	*r*	**0.741**	**0.325**					
	F	**67.098**	**6.487**					
	P	**<0.0001**	**0.014**					
log(Area X)	*r*	**0.569**	**0.461**	**0.678**				
	F	**26.288**	**14.827**	**46.920**				
	P	**<0.0001**	**0.0003**	**<0.0001**				
log(LMAN)	*r*	**0.398**	**0.432**	**0.497**	**0.717**			
	F	**10.373**	**12.593**	**18.037**	**58.275**			
	P	**0.002**	**0.0008**	**<0.0001**	**<0.0001**			
log(RA)	*r*	**0.461**	**0.446**	**0.702**	**0.698**	**0.699**		
	F	**14.836**	**13.695**	**53.386**	**52.272**	**52.645**		
	P	**0.0003**	**0.0005**	**<0.0001**	**<0.0001**	**<0.0001**		
log(DM)	*r*	0.141	0.237	0.222	0.190	0.101	0.197	
	F	1.108	3.260	2.851	2.056	0.562	2.224	
	P	0.297	0.076	0.097	0.157	0.456	0.142	
log(nXIIts)	*r*	0.176	0.122	**0.329**	**0.504**	**0.509**	**0.630**	0.163
	F	1.751	0.837	**6.658**	**18.766**	**19.224**	**36.278**	1.510
	P	0.191	0.364	**0.013**	**<0.0001**	**<0.0001**	**<0.0001**	0.224

Table S3. Multivariate PGLS models that explain variation in **log(syl rep)** as a function of various song nucleus volume combinations and the size covariate log(T-SS). R^2 values are not comparable to those from ordinary least squares models, and likelihood ratio tests are in comparison to the full model (#1).

		Parameter			Model				
Model	Nucleus	coef.	*F*	*P*	df	R^2	ln ML	AIC	LRT *P*
1	log(MMAN)	-0.178	0.148	0.702	39	0.723	-17.708	57.415	----
	log(Uva)	-0.358	0.134	0.716					
	log(HVC)	**2.999**	**41.087**	**<0.0001**					
	log(Area X)	-0.551	0.887	0.352					
	log(LMAN)	0.016	0.001	0.975					
	log(RA)	-1.129	2.262	0.141					
	log(DM)	0.337	0.165	0.687					
	log(nXIIts)	**-1.162**	**4.396**	**0.043**					
	log(T-SS)	0.619	0.622	0.435					
2	log(HVC)	**2.680**	**72.395**	**<0.0001**	44	0.710	-18.889	49.779	**0.797**
	log(RA)	**-1.440**	**5.898**	**0.019**					
	log(nXIIts)	**-1.159**	**6.038**	**0.018**					
	log(T-SS)	0.553	1.575	0.216					
3	log(HVC)	**2.803**	**60.063**	**<0.0001**	44	0.638	-24.284	60.567	0.022
	log(Area X)	-0.910	2.429	0.126					
	log(LMAN)	**-1.000**	**5.051**	**0.030**					
	log(T-SS)	-0.277	0.411	0.525					
4	log(MMAN)	**1.473**	**15.524**	**0.0003**	45	0.306	-40.240	90.481	<0.0001
	log(Uva)	0.918	0.829	0.367					
	log(T-SS)	-1.113	1.691	0.200					
5	log(MMAN)	0.020	0.002	0.967	45	0.482	-33.065	76.129	<0.0001
	log(HVC)	**1.826**	**16.424**	**0.0002**					
	log(T-SS)	**-0.969**	**4.153**	**0.047**					
6	log(MMAN)	**1.726**	**12.946**	**0.001**	45	0.302	-40.370	90.741	<0.0001
	log(Area X)	-0.433	0.586	0.448					
	log(T-SS)	-0.303	0.259	0.614					
7	log(MMAN)	**1.774**	**19.116**	**<0.0001**	45	0.331	-39.345	88.690	<0.0001
	log(LMAN)	-0.704	2.535	0.118					
	log(T-SS)	-0.202	0.132	0.719					
8	log(MMAN)	**1.660**	**16.100**	**0.0002**	45	0.306	-40.235	90.470	<0.0001
	log(RA)	-0.522	0.839	0.365					
	log(T-SS)	-0.127	0.036	0.851					
9	log(MMAN)	**1.499**	**15.572**	**0.0003**	45	0.293	-40.686	91.372	<0.0001
	log(DM)	-0.062	0.003	0.958					
	log(T-SS)	-0.467	0.276	0.602					
10	log(MMAN)	**1.631**	**21.469**	**<0.0001**	45	0.394	-36.908	83.816	<0.0001
	log(nXIIts)	**-1.360**	**7.506**	**0.009**					
	log(T-SS)	0.420	0.485	0.490					
11	log(Uva)	-0.965	1.083	0.304	45	0.494	-32.483	74.966	<0.0001
	log(HVC)	**1.964**	**38.070**	**<0.0001**					
	log(T-SS)	-0.421	0.365	0.549					

Table S3 (cont.)

		Parameter				Model			
Model	Nucleus	coef.	*F*	*P*	df	R^2	ln ML	AIC	LRT *P*
12	log(Uva)	1.394	1.526	0.223	45	0.135	-45.648	101.296	<0.0001
	log(nXIIts)	-1.111	3.537	0.066					
	log(T-SS)	0.637	0.421	0.520					
13	log(HVC)	**2.806**	**55.227**	**<0.0001**	45	0.597	-26.946	63.892	0.005
	log(Area X)	**-1.717**	**12.768**	**0.0009**					
	log(T-SS)	-0.305	0.458	0.502					
14	log(HVC)	**2.483**	**67.361**	**<0.0001**	45	0.618	-25.600	61.200	0.015
	log(LMAN)	**-1.426**	**16.031**	**0.0002**					
	log(T-SS)	-0.483	1.332	0.255					
15	log(HVC)	**2.904**	**83.403**	**<0.0001**	45	0.670	-22.040	54.080	**0.193**
	log(RA)	**-2.393**	**25.576**	**<0.0001**					
	log(T-SS)	0.400	0.756	0.389					
16	log(HVC)	**1.862**	**38.052**	**<0.0001**	45	0.485	-32.953	75.906	<0.0001
	log(DM)	-0.454	0.207	0.651					
	log(T-SS)	-0.694	0.843	0.363					
17	log(HVC)	**2.169**	**77.290**	**<0.0001**	45	0.671	-21.971	53.942	**0.202**
	log(nXIIts)	**-1.907**	**25.774**	**<0.0001**					
	log(T-SS)	0.182	0.174	0.679					
18	log(Area X)	**1.656**	**5.131**	**0.028**	45	0.144	-45.373	100.747	<0.0001
	log(LMAN)	-1.013	2.243	0.141					
	log(T-SS)	0.009	<0.001	0.989					
19	log(Area X)	**1.609**	**9.835**	**0.003**	45	0.266	-41.622	93.244	<0.0001
	log(nXIIts)	**-1.947**	**10.060**	**0.003**					
	log(T-SS)	0.768	1.373	0.248					
20	log(LMAN)	0.986	3.049	0.088	45	0.162	-44.859	99.717	<0.0001
	log(nXIIts)	**-1.818**	**6.196**	**0.017**					
	log(T-SS)	**1.383**	**4.453**	**0.040**					
21	log(RA)	**1.933**	**7.425**	**0.009**	45	0.232	-42.723	95.446	<0.0001
	log(nXIIts)	**-2.318**	**10.200**	**0.003**					
	log(T-SS)	0.609	0.738	0.395					
22	log(DM)	0.877	0.453	0.504	45	0.114	-46.219	102.439	<0.0001
	log(nXIIts)	-1.095	3.327	0.075					
	log(T-SS)	1.016	0.986	0.326					

Table S4. Residual analyses that explain variation in **log(syl rep)** as a function of relative song nucleus volumes. Volumes are either relative to another nucleus [e.g., HVC relative to RA, $HVC_{(RA)}$] or to the telencephalon minus the sum of song nuclei [e.g., $HVC_{(T\text{-}SS)}$]. SMP: song motor pathway (i.e. HVC+RA+nXIIts).

		Parameters				Model		
Model	Nucleus	coef.	*F*	*P*	df	R^2	ln ML	AIC
1	$HVC_{(RA)}$	**2.632**	**70.977**	**<0.0001**	46	0.693	-20.295	48.589
	$RA_{(nXIIts)}$	**1.418**	**12.508**	**0.0009**				
2	$HVC_{(RA)}$	**2.896**	**73.216**	**<0.0001**	47	0.609	-26.187	58.374
3	$RA_{(nXIIts)}$	**2.226**	**13.128**	**0.0007**	47	0.218	-43.161	92.322
4	$HVC_{(T\text{-}SS)}$	**1.840**	**36.467**	**<0.0001**	47	0.437	-35.126	76.251
5	$RA_{(T\text{-}SS)}$	0.467	0.606	0.440	47	0.013	-48.882	103.76
6	$nXIIts_{(T\text{-}SS)}$	-1.039	3.005	0.090	47	0.060	-47.678	101.35
7	$SMP_{(T\text{-}SS)}$	**1.897**	**21.512**	**<0.0001**	47	0.314	-39.963	85.926

Table S5. Residual analyses that explain variation in syllable repertoire size as a function of relative song nucleus neuron numbers.

		Parameters			Model			
Model	Nucleus	coef.	*F*	*P*	df	R^2	ln ML	AIC
1	$HVC\#_{(RA\#)}$	**2.371**	**66.517**	**<0.0001**	46	0.633	-24.662	57.324
	$RA\#_{(nXIIts\#)}$	**1.224**	**8.975**	**0.004**				
2	$HVC\#_{(RA\#)}$	**2.430**	**60.052**	**<0.0001**	47	0.561	-29.029	64.057
3	$RA\#_{(nXIIts\#)}$	**1.452**	**5.304**	**0.026**	47	0.101	-46.576	99.153
4	$HVC\#_{(T\text{-}SS)}$	**1.850**	**35.575**	**<0.0001**	47	0.431	-35.389	76.778
5	$RA\#_{(T\text{-}SS)}$	0.146	0.048	0.828	47	0.001	-49.171	104.34
6	$nXIIts\#_{(T\text{-}SS)}$	-1.233	2.805	0.101	47	0.056	-47.776	101.55
7	$SMP\#_{(T\text{-}SS)}$	**1.939**	**31.557**	**<0.001**	47	0.402	-36.611	79.222

Table S6. Two-factor PGLS models that explain variation in **log(syl rep)** as a function of a single structure volume or neuron number (#) and a corresponding size covariate. The partial *r*, coefficient, *F*-statistic and *P*-value refer to the relationship between each trait and repertoire size after accounting for size, while the ln ML and AIC values describe the entire model. In all cases, df = 46.

X		Trait				Model	
Size	Trait	*r*	coef.	*F*	*P*	ln ML	AIC
log(T-SS)	**log(MMAN)**	**0.510**	**1.496**	**16.145**	**0.0002**	**-40.687**	**89.375**
log(T-SS)	log(Uva)	0.150	1.186	1.056	0.310	-47.502	103.003
log(T-SS)	**log(HVC)**	**0.677**	**1.840**	**38.823**	**<0.0001**	**-33.066**	**74.131**
log(T-SS)	log(Area X)	0.243	0.841	2.889	0.096	-46.565	101.130
log(T-SS)	log(LMAN)	0.040	0.127	0.073	0.788	-48.019	104.038
log(T-SS)	log(RA)	0.116	0.467	0.622	0.434	-47.728	103.457
log(T-SS)	log(DM)	0.061	0.547	0.171	0.681	-47.967	103.933
log(T-SS)	log(nXIIts)	-0.251	-1.039	3.090	0.085	-46.465	100.929
log(T-SS)	**log(HVC#)**	**0.672**	**1.850**	**37.836**	**<0.0001**	**-33.352**	**74.704**
log(T-SS)	log(RA#)	0.033	0.146	0.049	0.826	-48.032	104.063
log(T-SS)	log(nXIIts#)	-0.243	-1.233	2.884	0.096	-46.568	101.135
log(Body Mass)	log(T)	0.183	1.430	1.589	0.214	-47.781	103.562
log(T-M)	log(M)	0.080	-0.680	0.293	0.591	-47.809	103.619
log(T-LS)	log(Hp)	0.113	-0.993	0.590	0.446	-47.680	103.360
log(T-LS)	log(Sep)	0.058	-0.561	0.153	0.697	-47.911	103.822
log(T-LS)	log(TnA)	0.117	-0.852	0.637	0.429	-47.656	103.311
log(T)	log(MLd)	0.021	0.141	0.021	0.885	-47.999	103.998

Spotted flycatcher
(*Muscicapa striata*)

Common yellowthroat
(*Geothlypis trichas*)

HVC

RA

1 mm

1 mm

caudal

d

m

l

v

rostral

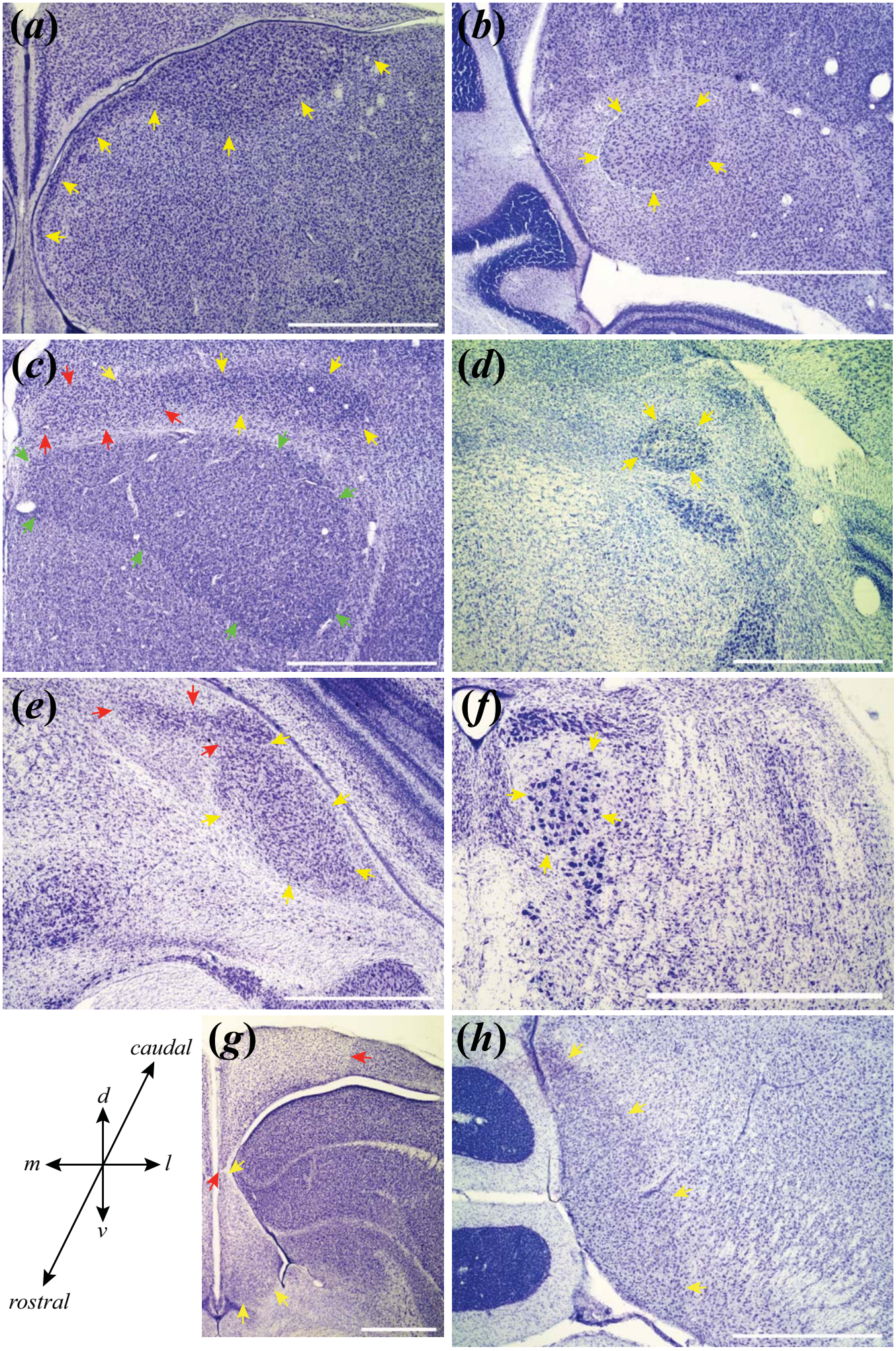
(a)
(b)
(c)
(d)
(e)
(f)
(g)
(h)
caudal
d
m
l
v
rostral